JACS
JOURNAL OF THE AMERICAN CHEMICAL SOCIETY
Communication
pubs.acs.org/JACS

Silica-Supported Cationic Gold(I) Complexes as Heterogeneous Catalysts for Regio- and Enantioselective Lactonization Reactions

Xing-Zhong Shu,[†,∥] Son C. Nguyen,[†] Ying He,[†] Fadekemi Oba,[†] Qiao Zhang,[†] Christian Canlas,[†] Gabor A. Somorjai,*[,†,‡,§] A. Paul Alivisatos,*[,†,§] and F. Dean Toste*[,†,‡]

[†]Department of Chemistry, University of California, Berkeley, California 94720, United States
[‡]Chemical Sciences Division and [§]Materials Sciences Division, Lawrence Berkeley National Laboratory, Berkeley, California 94720, United States
[∥]State Key Laboratory of Applied Organic Chemistry, and College of Chemistry and Chemical Engineering, Lanzhou University, Lanzhou 730000, P. R. China

Supporting Information

ABSTRACT: An efficient method for the synthesis of heterogeneous gold catalysts has been developed. These catalysts were easily assembled from readily available silica materials and gold complexes. The heterogeneous catalysts exhibited superior reactivity in various reactions where protodeauration is the rate-limiting step. Dramatic enhancement in regio- and enantioselectivity was observed when compared to the homogeneous unsupported gold catalyst. The catalysts are easily recovered and recycled up to 11 times without loss of enantioselectivity.

Integration of multiple catalytically relevant functionalities into a single active site is a concept often employed by biological catalysts (Scheme 1a)[1] and is an emerging strategy in heterogeneous[2] and homogeneous[3] catalysis. In an ideal scenario, the functional groups act cooperatively to enhance reactivity and/or selectivity.[4,5] The placement of a homogeneous catalyst in proximity to surface active sites of heterogeneous supports offers an opportunity exploit these cooperative effects while leveraging the benefits of both homogeneous and heterogeneous catalysis.[6] However, the use of this strategy to enhance the stability, reactivity, and enantioselectivity of chiral homogeneous catalysts remains illusive.

Scheme 1. Bifunctional Heterogeneous Molecular Catalyst

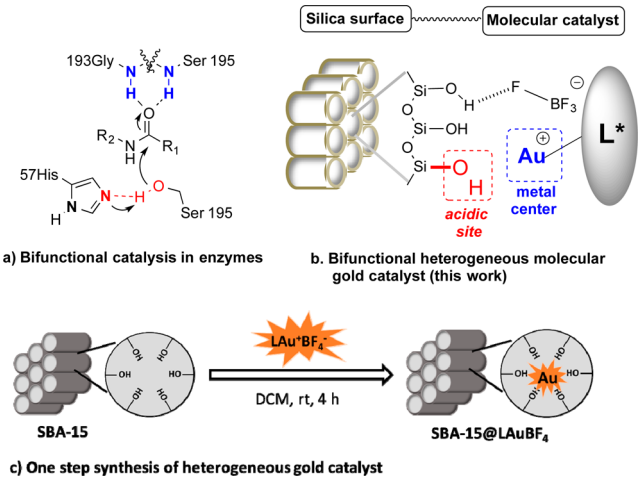

Homogeneous gold catalysts have proven to be both highly reactive and selective toward a variety of carbon−carbon and carbon−heteroatom bond forming reactions.[7] Inspired by recent reports showing that cationic metal complexes can be adsorbed onto mesoporous silica via hydrogen bonding of the counterion,[8] we envisioned that chiral cationic gold(I) complexes could be localized near the acidic silica surface to provide a bifunctional gold/Brønsted acid catalyst (Scheme 1b). Moreover, this process allows for a simple one-step synthesis from the homogeneous catalyst and retains the tunable electronic and steric properties of the original molecular catalyst.[9] Herein, we report the synthesis of a heterogeneous gold catalyst made by adsorbing molecular gold complexes onto mesoporous silica via such a hydrogen bonding method (Scheme 1b). More importantly, we show that the synergetic effect of the acidic silica surface significantly increases the catalyst's activity as well as regio- and enantioselectivity for intramolecular additions of allenes and alkynes.

The heterogeneous gold catalyst was prepared by stirring SBA-15 in a CH_2Cl_2 solution of Ph_3PAuBF_4 at room temperature for 4 h (Scheme 1c). The catalyst was separated by centrifugation, washed with CH_2Cl_2, and dried under vacuum to give a white solid, SBA-15@Ph_3PAuBF_4. The transmission electron microscope (TEM) images of SBA-15@Ph_3PAuBF_4 show a regular hexagonal array of uniform channels that is characteristic of mesoporous SBA-15 materials (Figure 1a). The catalyst was treated with ascorbic acid to reduce the homogeneous gold complex and enable the direct observation of the gold nanoparticles. Gold nanoparticles formed during the reduction by ascorbic acid are clearly seen inside the mesoporous channels, indicating the successful adsorption of the catalyst onto the pores (Figure 1b). This conclusion was further confirmed through nitrogen sorption experiments. Compared to SBA-15, SBA-15@Ph_3PAuBF_4 showed less

Received: April 27, 2015
Published: May 29, 2015

DOI: 10.1021/jacs.5b04294
J. Am. Chem. Soc. 2015, 137, 7083−7086

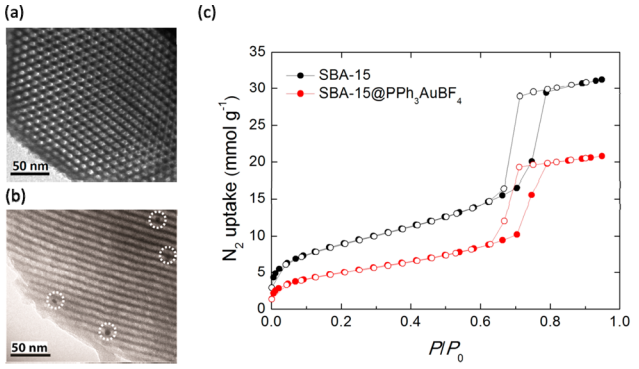

Figure 1. TEM image of (a) heterogeneous catalyst SBA-15@Ph_3PAuBF_4; (b) SBA-15@Ph_3PAuBF_4 after treatment with ascorbic acid to reduce Au^+ to gold nanoparticles (dark spots). (c) Nitrogen sorption isotherms for SBA-15 (black) and catalyst SBA-15@Ph_3PAuBF_4 (red) at 77 K with adsorption and desorption branches represented by closed and open circles, respectively. P/P_0, relative pressure.

surface area and smaller pores (Figure 1c), consistent with the presence of molecular catalysts in the mesopores. The type IV isotherm with a H1 hysteresis loop indicates that the heterogeneous catalysts retain the ordered mesoporous channels of SBA-15.

The preservation of the molecular catalyst's structure in SBA-15@Ph_3PAuBF_4 was further demonstrated by IR spectroscopy (Figure 2). In addition, a significant red shift of the O–H

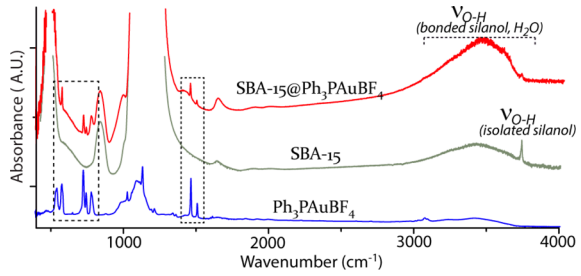

Figure 2. FTIR spectra of molecular catalyst Ph_3PAuBF_4 (blue), silica material SBA-15 (gray), and heterogeneous catalyst SBA-15@Ph_3PAuBF_4 (red). All observable absorption bands of the catalyst loaded in SBA-15 precisely resembled the spectra of the original catalyst.

stretching vibrational band at 3750 cm^{-1} in SBA-15@Ph_3PAuBF_4 was observed, consistent with hydrogen bonding of the surface silanol groups in SBA-15 with the molecule catalyst.

The existence of this hydrogen bond was also investigated using ^{19}F MAS NMR spectroscopy (Figure 3). Three major

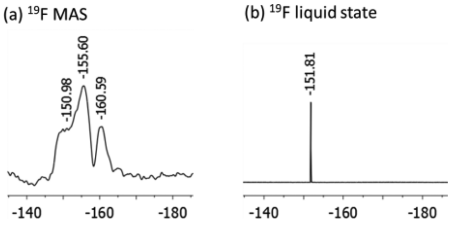

Figure 3. (a) ^{19}F MAS NMR spectra of SBA-15@Ph_3PAuBF_4; (b) ^{19}F NMR spectra of Ph_3PAuBF_4 in CD_3CN.

resonances were detected in SBA-15@Ph_3PAuBF_4 at −152, −156, and −160 ppm while the homogeneous counterpart only showed a single resonance at −152 ppm in a solution ^{19}F NMR spectrum. On the basis of previously reported values, the resonances observed in the SBA-15@Ph_3PAuBF_4 sample were are assigned as follows: −156 ppm (F in BF_4^- hydrogen bonded to the surface silanol group), −152 ppm (F in BF_4^- not hydrogen bonded), and −162 ("bulk" BF_4^- species).[10] The observation of these characteristic peaks further validates the hypothesis that the gold complex was immobilized on the silica surface by hydrogen bonding of the BF_4^- anion to surface silanol groups in SBA-15.

Previous studies have revealed that protodeauration of a vinylgold intermediate (**3**) is the turnover limiting, and often selectivity defining, step in gold-catalyzed addition of oxygen nucleophiles to allenes.[11] On the basis of these reports, we examined their reactivity of the silica-supported gold catalysts in the lactonization reaction of allenoic acid **1a**. The heterogeneous gold catalyst SBA-15@Ph_3PAuBF_4 exhibited superior activity compared to its homogeneous counterpart under the same conditions (eq 1a vs b).[12] Thus, we propose that the

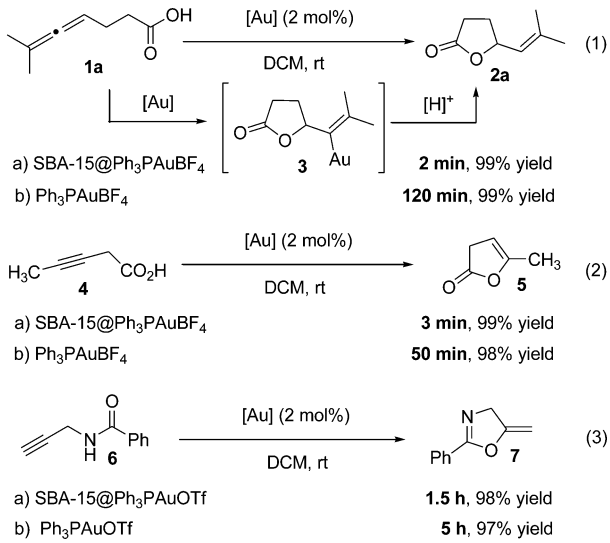

enhanced reactivity of SBA-15@Ph_3PAuBF_4 is likely due to enhancement of protodeauration by the surface acidity of silica (**3** to **2a**). A series of reactions with the same rate-limiting step was also found to be accelerated by introducing molecular gold catalysts into SBA-15 (eqs 2 and 3).

Reactions in the silica mesopores gave a different selectivity than those occurring in solution.[13] The cyclization of alkynoic acid was then studied, and the regioselectivity obtained from SBA-15@Ph_3PAuBF_4 is 3 times greater than that of the homogeneous counterpart (Scheme 2 a–c). By introducing substituents at the α-carbon of the acid, the 5-exo cyclization products were obtained, with 100% purity using a heterogeneous gold catalyst (Scheme 2d–e).

We next examined the application of the supported catalysts system to the transition-metal-catalyzed enantioselective nucleophilic addition reactions of allenes. Although intramolecular hydroamination and -alkoxylation of allenes have been well established,[14] the lactonization reactions remain challenging.[15] The unique feature of our method is that chiral heterogeneous gold catalysts are easily assembled from readily available molecular catalysts, thereby allowing for rapid catalysts assessment. Thus, a series of heterogeneous gold catalysts with

DOI: 10.1021/jacs.5b04294
J. Am. Chem. Soc. 2015, 137, 7083–7086

Scheme 2. Regioselectivity Studies of the Synthesized Heterogeneous Gold Catalysts

substrate	Ph_3PAuBF_4	SBA-15@Ph_3PAuBF_4
a) $R^1 = CH_3$, $R^2 = H$ (**8a**)	1.5 : 1	4 : 1
b) $R^1 = H$, $R^2 = H$ (**8b**)	3 : 1	9 : 1
c) $R^1 = Cl$, $R^2 = H$ (**8c**)	6 : 1	18 : 1
d) $R^1 = H$, $R^2 = CH_3$ (**8d**)	20 : 1	100 : 0
e) $R^1 = Cl$, $R^2 = CH_3$ (**8e**)	35 : 1	100 : 0

different chiral phosphine ligands were prepared and explored as catalysts for the enantioselective hydrocarboxylation of allenoic acid **1a** (Table 1). Although no enantioselectivity was

Table 1. Optimization of Gold-Catalyzed Enantioselective Cyclization of Allenoic Acid[a]

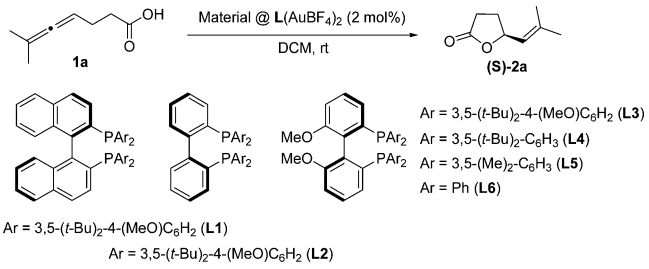

entry	catalyst	yield (%)[b]	ee (%)[d]
1	**L1**$(AuBF_4)_2$	91	0
2	SBA-15@**L1**$(AuBF_4)_2$	93	66
3	SBA-15@**L2**$(AuBF_4)_2$	95	52
4	SBA-15@**L3**$(AuBF_4)_2$	92	75
5	SBA-15@**L4**$(AuBF_4)_2$	92	48
6	SBA-15@**L5**$(AuBF_4)_2$	93 (87)[c]	84
7	SBA-15@**L6**$(AuBF_4)_2$	94	47
8	MCM-41@**L5**$(AuBF_4)_2$	95	81
9	micelle@**L5**$(AuBF_4)_2$	93	81
10	**L5**$(AuBF_4)_2$ + nonmesoporous silica	90	50

[a]Reaction works at rt using **1a** (0.1 mmol), catalyst (2 mol %) in DCM (2 mL). [b]Yields were calculated based on ^1H NMR using internal standard. [c]Isolated yield. [d]Determined by chiral HPLC.

obtained using molecular gold complexes as a homogeneous catalyst, gold complexes adsorbed on SBA-15 all exhibit considerable enantioselectivity. Among them, the BIPHEP ligand stood out as most effective (entries 2–4). While a less electron-rich ligand did not enhance the selectivity (entry 5), a decrease in the ligand size significantly improved the enantioselectivity and gave (*S*)-**2a**[16] in 84% ee (entry 6). However, a further decrease in sterics of the ligand gave an inferior result (entries 7).

The versatility of heterogeneous catalyst SBA-15@L5-$(AuBF_4)_2$ toward cyclization of various allenoic acids was further studied (Table 2). When a dimethyl group was introduced at the α-position of the acid, the enantioselectivity was increased (**2b** and **2c**). A 93% ee was obtained for the synthesis of six-membered lactone **2d**. Both linear and cyclic substituents in the allenoic were tolerated (**2e** and **2f**).

Table 2. Enantioselective Lactonization of Allenoic Acid Catalyzed by Heterogeneous Gold Catalyst

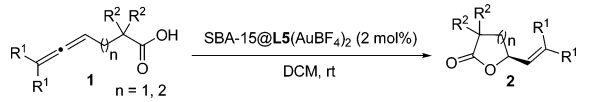

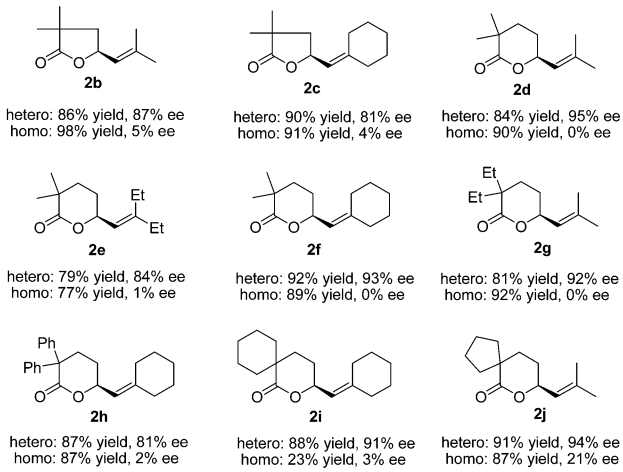

Substituents at the α-carbon of allenoic acid could be alkyl, aryl, and unsaturated rings (**2g–2j**). Low enantioselectivities were obtained in the presence of a homogeneous catalyst in all cases.

Silica materials with varying pore size and particle morphology demonstrated analogous behaviors to those observed of SBA-15. For example, similar enantioselectivity was achieved in the lactonization of **1a** catalyzed by MCM-41@ L5$(AuBF_4)_2$ and micelle@L5$(AuBF_4)_2$[17] (Table 1, entries 8 and 9). On the other hand, the combination of the chiral gold catalyst and silica in which the pores are occupied by cetyltrimethylammonium bromide (CTAB) produced lactone **2a** with lower enantioselectivity. While confinement[18] of the catalyst in the mesopore may enhance selectivity, the observation that the structure of the support has little impact on enantioselectivity suggests that the cooperative effect of surface silanols is primarily responsible for the observed enhancements in selectivity.

In order to take advantage of its heterogeneous nature, the recyclability of the catalyst SBA-15@L5$(AuBF_4)_2$ was investigated. The catalyst was easily recovered from the solution by centrifugation and used for the next catalytic cycle without any additional treatment. No decrease in the enantioselectivity was observed for 11 cycles (Table S1). The stability of the catalyst SBA-15@L5$(AuBF_4)_2$ was also studied by FTIR spectroscopy, which showed that 63% of molecular catalyst was left after 11 runs (Figure S8). Moreover, Inductively Coupled Plasma Optical Emission Spectroscopy (ICP-OES) analysis revealed 3.2% total leaching of the gold complex after 11 runs. The observation of Au nanoparticles inside mesoporous silica after 11 runs suggests that part of cationic catalyst loss is due to reduction to gold(0).

In conclusion, we have developed an efficient method for the synthesis of heterogeneous gold catalysts. The tunable catalysts can be easily assembled from readily available silica supports and cationic gold(I) complexes. Compared with homogeneous catalysts, the heterogeneous gold catalysts exhibited superior catalytic activity toward various reactions with protodeauration as the rate-limiting step, and showed significant enhancement

DOI: 10.1021/jacs.5b04294
J. Am. Chem. Soc. 2015, 137, 7083–7086

in regio- and enantioselectivity. More importantly, the present work highlights the potential of ionic interactions with charged catalysts as a strategy for rapid assembly and assessment of cooperative effects between supports and chiral homogeneous catalysts for the develop of heterogeneous asymmetric catalysts.

■ ASSOCIATED CONTENT

Supporting Information

Details of experimental procedures, NMR spectra, and spectroscopic data. The Supporting Information is available free of charge on the ACS Publications website at DOI: 10.1021/jacs.5b04294.

■ AUTHOR INFORMATION

Corresponding Authors

*somorjai@berkeley.edu (G.A.S.)
*alivis@berkeley.edu (A.P.A.)
*fdtoste@berkeley.edu (F.D.T.)

Notes

The authors declare no competing financial interest.

■ ACKNOWLEDGMENTS

We thank the financial support from the Dow Chemical Company through funding for the Core−Shell Catalysis Project, Contract No. 20120984 to University of California, Berkeley. We are grateful to Dr. David Barton, Dr. Pete Nickias, and Dr. Trevor Ewers from Dow Chemical Co.; Dr. Elad Gross and Juncong Jiang for useful discussions; Julia Oktawiec for the nitrogen adsorption−desorption isotherms; and Rong Ye for Inductively Coupled Plasma Optical Emission Spectroscopy (ICP-OES) analysis.

■ REFERENCES

(1) (a) Ringe, D.; Petsko, G. A. *Science* **2008**, *320*, 1428−1429. (b) warshel, A.; Sharma, P. K.; Kato, M.; Xiang, Y.; Liu, H.; Olsson, M. H. M. *Chem. Rev.* **2006**, *106*, 3210−3235.

(2) (a) Margelefsky, E. L.; Zeifan, R. K.; Davis, M. E. *Chem. Soc. Rev.* **2008**, *37*, 1118−1126. (b) Notestein, J. M.; Katz, A. *Chem.—Eur. J.* **2006**, *12*, 3954−3965. (c) Yu, C.; He, J. *Chem. Commun.* **2012**, *48*, 4933−4940. (d) Kung, H. H.; Kung, M. C. *Catal. Today* **2009**, *148*, 2−5.

(3) (a) Xu, H.; Zuend, S. J.; Wolf, M. G.; Tao, Y.; Jacobsen, E. N. *Science* **2010**, *327*, 986−990. (b) Matsunaga, S.; Shibasaki, M. *Chem. Commun.* **2014**, *50*, 1044−1057. (c) Park, J.; Hong, S. *Chem. Soc. Rev.* **2012**, *41*, 6931−6943.

(4) For an example of a support-enhanced reaction of supported organocatalysts, see: (a) Motokura; Tada, M.; Iwasawa, Y. *J. Am. Chem. Soc.* **2007**, *129*, 9540−9541. (b) Shylesh, S.; Thiel, W. *ChemCatChem* **2011**, *3*, 278−287. (c) Motokura, K.; Tada, M.; Iwasawa, Y. *Chem.—Asian J.* **2008**, *3*, 1230−1236.

(5) For examples with cooperative catalysis with transition metals attached to surfaces via tethered ligands, see: (a) Noda, H.; Motokura, K.; Miyaji, A.; Baba, T. *Angew. Chem., Int. Ed.* **2012**, *124*, 8141−8144. (b) Deiana, L.; Ghisu, L.; Afewerki, S.; Werho, O.; Johnston, W. V.; Hedin, N.; Bacsik, Z.; Córdova, A. *Adv. Synth. Catal.* **2014**, *356*, 2485−2492. With metal nanoparticles, see: (c) Choo, G. C. Y.; Miyamura, H.; Kobayashi, S. *Chem. Sci.* **2015**, *6*, 1719−1727 and references therein.

(6) (a) Tada, M.; Kotokura, K.; Iwasawa, Y. *Top. Catal.* **2008**, *48*, 32−40. (b) Askevoid, B.; Roesky, H. W.; Schneider, S. *ChemCatChem* **2012**, *4*, 307−320. (c) Gross, E.; Toste, F. D.; Somorjai, G. A. *Catal. Lett.* **2015**, *145*, 126−138.

(7) For selected reviews on homogeneous gold catalysis, see: (a) Obradors, C.; Echavarren, A. M. *Chem. Commun.* **2014**, *50*, 16−28. (b) Garayalde, D.; Nevado, C. *ACS Catal.* **2012**, *2*, 1462−1479. (c) Rudolph, M.; Hashmi, A. S. K. *Chem. Soc. Rev.* **2012**, *41*, 2448−2462. (d) Gorin, D. J.; Toste, F. D. *Nature* **2007**, *446*, 395−403. For reviews on enantioselective gold catalysis, see: (e) Wang, Y.-M.; Lackner, A. D.; Toste, F. D. *Acc. Chem. Res.* **2014**, *47*, 889−901. (f) Sengupta, S.; Shi, X. *ChemCatChem* **2010**, *2*, 609−619.

(8) For application of this method in Rh-catalyzed hydrogenation reactions: (a) de Rege, F. M.; Morita, D. K.; Ott, K. C.; Tumas, W.; Broene, R. D. *Chem. Commun.* **2000**, 1797−1798. (b) Raja, R.; Thomas, J. M.; Jones, M. D.; Johnson, B. F. G.; Vaughan, D. E. W. *J. Am. Chem. Soc.* **2003**, *125*, 14982−14983. Rh-catalyzed hydroformylation: (c) Bianchini, C.; Burnaby, D. G.; Evans, J.; Frediani, P.; Meli, A.; Oberhauser, W.; Psaro, R.; Sordelli, L.; Vizza, F. *J. Am. Chem. Soc.* **1999**, *121*, 5961−5971. Cu-catalyzed alkynylation reactions: (d) McDonagh, C.; O'Conghaile, P.; Gebbink, R. J. M. K.; O'Leary, P. *Tetrahedron Lett.* **2007**, *48*, 4387−4390. Diels−Alder reactions: (e) Wang, H.; Liu, X.; Xia, H.; Liu, P.; Gao, J.; Ying, P.; Xiao, J.; Li, C. *Tetrahedron* **2006**, *62*, 1025−1032.

(9) For alternative approaches to enantioselective heterogeneous gold catalysis, see: (a) Gross, E.; Liu, J. K.; Alayoglu, S.; Marcus, M. A.; Fakra, S. C.; Toste, F. D.; Somorjai, G. A. *J. Am. Chem. Soc.* **2013**, *135*, 3881−3886. For recent reviews on enantioselective heterogeneous catalysis, see: (b) Yasukawa, T.; Miyamura, H.; Kobayashi, S. *Chem. Soc. Rev.* **2014**, *43*, 1450−1461. (c) Fraile, J. M.; Garcia, J. I.; Herrerias, C. I.; Mayoral, J. A.; Pires, E. *Chem. Soc. Rev.* **2009**, *38*, 605−706.

(10) Wiench, J. W.; Michon, C.; Ellern, A.; Hazendonk, P.; Iuga, A.; Angelici, R. J.; Pruski, M. *J. Am. Chem. Soc.* **2009**, *131*, 11801−11810.

(11) Brown, T. J.; Weber, D.; Gagné, M. R.; Widenhoefer, R. A. *J. Am. Chem. Soc.* **2012**, *134*, 9134−9137.

(12) See Supporting Information for control experiments examining the accelerating effect of a Brønsted acid (Figure S7).

(13) Gross, E.; Liu, J. H.; Toste, F. D.; Somorjai, G. A. *Nat. Chem.* **2012**, *4*, 947−952.

(14) (a) Arbour, J. L.; Rzepa, H. S.; Contreras-García, J.; Adrio, L. A.; Barreiro, E. M.; Hii, K. K. *Chem.—Eur. J.* **2012**, *18*, 11317−11324. (b) LaLonde, R. L.; Sherry, B. D.; Kang, E. J.; Toste, F. D. *J. Am. Chem. Soc.* **2007**, *129*, 2452−2453. (c) Zhang, Z.; Bender, C. F.; Widenhoefer, R. A. *J. Am. Chem. Soc.* **2007**, *129*, 14148−14149. (d) Zhang, Z.; Widenhoefer, Z. R. A. *Angew. Chem., Int. Ed.* **2007**, *46*, 283−285. (e) Hamilton, G. L.; Kang, E. J.; Mba, M.; Toste, F. D. *Science* **2007**, *317*, 496−499. (f) Teller, H.; Corbet, M.; Mantilli, L.; Gopakumar, G.; Goddard, R.; Thiel, W.; Fürstner, A. *J. Am. Chem. Soc.* **2012**, *134*, 15331−15342.

(15) Handa, S.; Lippincott, D. J.; Aue, D. H.; Lipshutz, B. H. *Angew. Chem., Int. Ed.* **2014**, *53*, 10658−10662.

(16) The absolute configuration of product **2a** was determined by comparison with the known reference structure in ref 15.

(17) Zhang, Q.; Shu, X.-Z.; Lucas, J. M.; Toste, F. D.; Somorjai, G. A.; Alivisatos, A. P. *Nano Lett.* **2014**, *14*, 379−383.

(18) For reviews of confinement effects in catalysis, see: (a) Song, C. E.; Kim, D. H.; Choi, D. S. *Eur. J. Inorg. Chem.* **2006**, 2927−2935. (b) Goettmann, F.; Sanchez, C. *J. Mater. Chem.* **2007**, *17*, 24−30. For examples in gold(I) catalysis, see: (c) Wang, Z. J.; Brown, C. J.; Bergman, R. G.; Raymond, K. N.; Toste, F. D. *J. Am. Chem. Soc.* **2011**, *133*, 7358−7360. (d) Cavarzan, A.; Scarso, A.; Sgarbossa, P.; Strukul, G.; Reek, J. N. H. *J. Am. Chem. Soc.* **2011**, *133*, 2848−2852. (e) Adriaenssens, L.; Escribano-Cuesta, A.; Homa, A. M.; Echavarren, A. M.; Ballester, P. *Eur. J. Org. Chem.* **2013**, 1494−1500.

DOI: 10.1021/jacs.5b04294
J. Am. Chem. Soc. 2015, 137, 7083−7086